Controlled by the permittivity transformation of energy bands of dielectric metamaterial arrays

A. Hosseinzadeh, E. Semouchkina, and G. Semouchkin

Department of Electrical and Computer Engineering
Michigan Technological University
Houghton, MI, 49931, USA
Fax: + 1-906-487-2949; email: esemouch@mtu.edu

Abstract

Band diagrams of 2D arrays of dielectric rods are simulated at TE wave incidence in dependence on dielectric permittivity of rod material. It is shown that permittivity defines the variety of propagation modes corresponding to extreme energies of the lowest transmission bands because of interplay between Bragg and Mie resonances.

1. Introduction

Among various types of resonance structures proposed to build metamaterials, arrays of dielectric resonators present a special interest because of lower loss and better scaling perspectives for operation at higher frequencies. At the same time, dielectric arrays are conventionally used to form photonic crystals (PCs). This paper aims to bridge two approaches to analysing dielectric resonator arrays and investigates the specifics of their energy band diagrams in dependence on the permittivity of the dielectric rods.

Since metamaterials are assumed homogenized only if the wavelengths of the incident wave essentially exceeds both the lattice parameter and the size of resonators, the range of the relative permittivity values for the rod material ε has been chosen varying from 10 to 50, while the range of the filling factor $\beta = r/a$, where r is the radius of the cylindrical resonator and $\alpha -$ the lattice parameter, is considered changing in the range from 0.1 to 0.4. These ranges ensured that at $\varepsilon = 50$ and $\beta = 0.4$ both α and the diameter of resonators ϕ were almost 10 times smaller than the incident wavelength in air and, so, corresponded to the metamaterial criteria. From the other hand, at $\varepsilon = 25$ and $\beta = 0.1$ the parameter α appears to be equal to the half wavelength in air that is close to the PC criteria, even though ϕ value still remains to be much smaller than the wavelength. The chosen ranges of the array parameters, therefore, covered the transition from PC to metamaterials. In order to provide better alignment with PC studies, 2D arrays of infinite dielectric rods were investigated first, which are known as convenient PC constituents because of the possibility to separate TE and TM excitation options and to extract band diagrams in a straightforward way [1]. Previously, it was shown in [2] that dielectric rods at TE excitation can demonstrate magnetic type response. This response, therefore, could be compared with the response of metamaterial arrays of dielectric resonators.

2. Investigation approaches

Infinitely long dielectric cylindrical rods were arranged in square lattices in air with their axes normal to the XY plane (Fig. 1). Incident plane wave was propagating along X axis with the magnetic field

ISBN 978-952-67611-2-1

vector directed along Z axis and electric field vector - along Y axis. For the chosen TE mode excitation analysis of band diagrams was limited by the ΓX direction. Band diagrams were extracted by using the MPB software developed for PC studies [3].

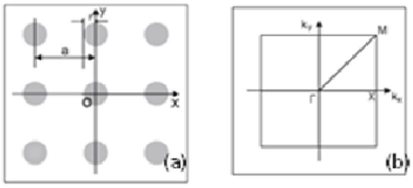

Fig. 1. (a) Cross section of a square lattice of rods with radius "r" and lattice constant "*a* "; (b) first Brillouin zone (BZ) of the array, where Γ, X and M are symmetry points.

In order to compare results for arrays with various lattice parameters, the invariance of Maxwell's equations for objects with n-times changed dimensions at n-times decreased or increased frequencies was taken into account. Therefore, the lattice constant "*a*" was used as the unit of length and all angular frequencies ω were expressed as multiples of $\frac{2\pi c}{a}$ (c is the speed of light). Employment of this frequency measure made the above listed multiples equal to the value of $\frac{a}{\lambda}$, where λ is the wavelength in vacuum. In accordance with Bloch-Floquet theorem, the search for unique data could be limited by the k range of $\frac{2\pi}{a}$, i.e. from $-\frac{\pi}{a}$ to $\frac{\pi}{a}$ (within the first Brillouin zone). Due to the symmetry of the problem the k-range could be additionally reduced: from 0 to $\frac{\pi}{a}$. All wave numbers were normalized with respect to $\frac{\pi}{a}$.

An example of calculation results for the band diagram of a square lattice composed from dielectric rods with $\beta = 0.2$ and ε=10 is shown in Fig. 2a. To verify the obtained data, they were compared with the transmission spectrum calculated for the array under study by using the CST MW Studio commercial software (Fig. 2b). As seen in the figure, both methods provided the same positions of stop bands in the energy spectrum. This result additionally justified determination of extreme energy values for the array transmission bands by using the positions of points A-D in the band diagram.

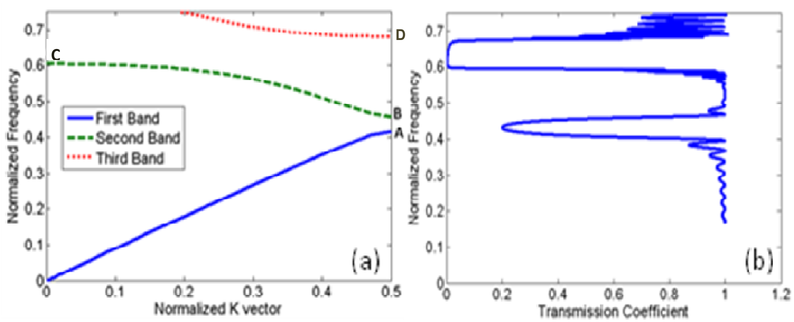

Fig. 2. (a) Band diagram and (b) transmission spectrum for the square lattice of rods with r=0.2a and $\varepsilon = 10$.

3. Transformation of energy bands in dependence on the rod material permittivity

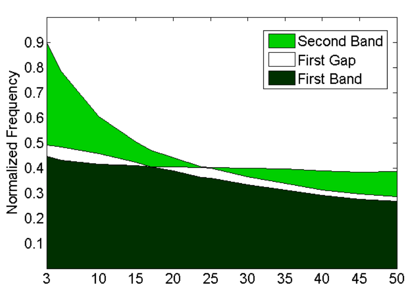

Fig. 3. Energy bands of arrays with $\beta = 0.2$ versus rod permittivity.

Fig. 3 presents extreme frequencies of the 1st and 2nd transmission bands of rod arrays with $\beta = 0.2$ in dependence on the rod material permittivity. Dependencies with similar specifics but shifted right ($\beta = 0.1$) or left along the permittivity axis were observed for other β values. As seen in the figure, extreme frequencies decay at the permittivity increase so that the band gap closes at some point $\varepsilon = \varepsilon_A$ (depending on the filling factor), while the 2nd transmission band closes at another point $\varepsilon = \varepsilon_B$. Some hints for understanding the nature of the described above transformations were obtained at investigating the propagation modes corresponding to the extreme frequencies of the 1st and the 2nd transmission bands. These modes were characterized by amplitude distributions of Hz field in the XY cross-section of the structure. They were numbered in the order of appearance at increasing energy in the band diagrams for arrays with the rod permittivity $\varepsilon = 10$. As seen in Fig. 4, the 1st mode features maximal field intensity between the rods along the lines normal to the wave propagation direction, while the 2nd and the 3rd modes feature fields confined within the rods. The 2nd mode displays opposite phases of field oscillations confined in every other rod line. The 3rd mode features coherent oscillations in all rods.

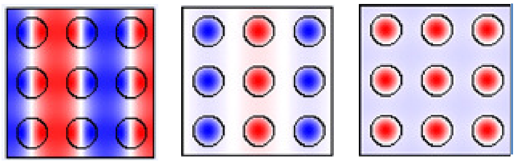

Fig. 4. Field profiles of the propagation modes in the 1st and 2nd transmission bands.

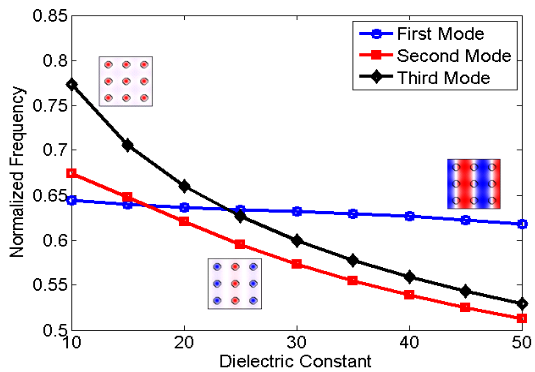

Fig. 5. Normalized frequency of three propagation modes versus permittivity for r=0.2a.

Fig. 5 illustrates changes of frequencies, at which the above modes can be observed in arrays. These changes for the 2nd and the 3rd modes are represented by almost conformal decaying curves, while changes of the 1st mode frequency are described by the line crossing the curves for two other modes. The crossings occur at the same ε_A and ε_B, at which the closings of the gap and the second transmission band have been observed in Fig. 3. This makes the 1st mode appear at the upper edge of the 1st transmission band for $\varepsilon < \varepsilon_A$, at the lower edge of the 2nd transmission band for $\varepsilon_A < \varepsilon < \varepsilon_B$, and at the upper edge of the 2nd transmission band for $\varepsilon > \varepsilon_B$. It is worth noting that a weak dependence of the 1st mode frequency on the rod permittivity and its field profile look characteristic for the Bragg resonance. Appearance of this mode just below the first gap in the band diagrams of arrays with low permittivity also confirms its Bragg's origin, since this gap is usually related to Bragg's resonance in PCs. In such case, appearance of the 1st mode just below the second gap in the band diagrams of arrays with high rod permittivity could point out at Bragg's origin of the respective gap in metamaterial arrays. From the other hand, the 2nd and the 3rd modes, especially at high rod permittivity, seem to be related to Mie-resonances in the rods. These resonances apparently define the first gap in the band diagrams of arrays with rod permittivity $\varepsilon > \varepsilon_B$ due to the negativity of the resonance controlled effective permeability of the medium at $f > f_{res}$. Field profile of the 2nd and the 3rd modes testify in favour of such suggestion as they look similar to the so called "bonding" and "anti-bonding" resonance modes observed near the transmission gap edges in arrays of dielectric resonators [4]. More complicated situation takes place at $\varepsilon_A < \varepsilon < \varepsilon_B$, where both Bragg and Mie resonances are involved at the same energies.

4. Conclusion

It is demonstrated that band diagrams of metamaterials composed from dielectric rods experience significant transformations in dependence on the permittivity of rod material. These transformations are shown to result from the interplay between Bragg and Mie resonances.

References

[1] J. D. Joannopoulos, S. G. Johnson, J. N.Winn, and R. D. Meade, *Photonic Crystals, Molding the Flow of Light*, Princeton, NJ: Princeton Univ. Press, 2008.
[2] S. O'Brien and J. B. Pendry, Photonic band-gap effects and magnetic activity in dielectric composites, *J. Phys.: Cond. Matter*, vol. 14, p. 4035, 2002.
[3] S. G. Johnson and J. D. Joannopoulos, Block-iterative frequency-domain methods for Maxwell's equations in a planewave basis, *Optics Express* 8, No. 3, p. 173, 2001.
[4] A. Hosseinzadeh and E. Semouchkina, Coupling of elementary resonances in 3D metamaterials, Proceeding of *IEEE AP-S Int. Symp.*, Spokane, WA, p. 2593 , 2011.